Utah State University

DigitalCommons@USU

12-2013

An Analysis on Soil Properties on Predicting Critical Hydraulic Gradients for Piping Progression in Sandy Soils

Tammy Jacobson
Utah State University

UtahState University
MERRILL-CAZIER LIBRARY

UTAH STATE UNIVERSITY

An Analysis on Soil Properties on Predicting Critical Hydraulic Gradients for Piping Progression in Sandy Soils

A project submitted in partial fulfillment of the requirements for the degree of
Master of Science
in
Civil Engineering

Tammy Jacobson

12/12/2013

Approved:

_____
Dr. John Rice
Major Professor

_____
Dr. James A. Bay
Committee Member

_____
Dr. Gilberto Urroz
Committee Member

ABSTRACT

An Analysis on Soil Properties on Predicting Critical Hydraulic Gradients for
Piping Progression in Sandy Soils

By

Tammy Jacobson, Master of Science
Utah State University 2013

Major Professor: Dr. John Rice
Department: Civil and Environmental Engineering

Piping is a form of internal erosion in which soil particles are eroded at a seepage exit location due to the forces imposed on the particles by seeping water. Laboratory testing was performed on a variety of soils in order to assess a correlation between unit weight, angle of internal friction, grain size, gradation, and void ratio and the critical hydraulic gradient at which piping initiates and progresses. A multi-variable regression analysis was used to form equations to predict critical hydraulic gradient based upon each of these soil parameters. Variations in the accuracy of these equations are thought to be due to the interlocking behavior of the angular soils tested compared to that of the more spherical soils as well as the loosening of the sample and change in void ratio as piping progresses.

Introduction

Internal erosion includes several different mechanisms. These include heave, piping, concentrated leak erosion, contact erosion and suffusion (ICOLD 2012). Internal erosion accounts for nearly half of all world-wide dam and levee failures, with nearly one-third of all piping failures being associated with the backwards erosion model of piping (Richards and Reddy 2007). Piping is often described using the term backward erosion. This is because piping is the erosion of soil particles at some seepage exit location due to forces imposed by water transport through a porous media. This process results in channels or "pipes" that progress in an upward gradient back towards the water source (Richards and Reddy 2007). This occurs as the result of high hydraulic gradients of velocities.

Attempts have been made to quantify the hydraulic conditions needed to initiate piping failure. The theory of heave was proposed by Terzaghi (1922, 1939, 1943). His theory is consistent with Darcy Law assumptions in which flow takes place vertically through a horizontal face. His equation for the critical gradient (Equation 1) at which heave occurs under this condition is the ratio of the buoyant unit weight of the soil (γ') to the unit weight of water (γ_w).

$$i_{cr} = \frac{\gamma'}{\gamma_w} \qquad\qquad (1)$$

Terzaghi and Peck differentiated between heave and piping. They noted that piping and piping failures were the result of subsurface erosion; however this phenomenon of subsurface erosion was termed to "defy theoretical approach" (Terzaghi and Peck 1948, Richards and Reddy 2007). While the heave theory is limited, some form of Terzaghi's heave theory is commonly used to predict factor of safety against piping.

It is likely that critical gradients for piping failure to occur involve factors other than the buoyant unit weight of the soil. These factors could include but are not limited to the particle size and gradation of the soil, soil friction angle, particle to particle interaction, and void ratio. This paper attempts to quantify the effects of these soil characteristics by generating an equation for critical gradient as a result of soil unit weight, friction angle, particle size, gradation, and void ratio using results from laboratory testing on cohesionless soils. The results of this analysis will be presented in relation to the different stages noted by Fleshman and Rice in their laboratory models (Fleshman and Rice 2013).

Background of Piping Studies

The first theories related to piping failures were developed by Bligh (1910, 1913). Bligh recognized a possible relationship between the length of the flow path and the forces available to move soil particles. He derived an empirical method for evaluating piping near the contact between structures and soils known as the line-of creep theory in which the flow path is the summation of the vertical and horizontal distances along the contact plane (Richards and Reddy 2007). Bligh's line-of-creep theory was improved upon by Lane in 1934. Lane distinguished between flow along a structure-soil contact and flow through granular media to develop the weighted-creep-method. Lane's methodology assumed anisotropic flow which reduced the length of the horizontal flow paths. His use of safe weighted creep ratios took into account variances in erosion resistance in different soil types (Richards and Reddy 2007).

Researchers have attempted to correlate piping mechanisms with various soil properties. Flume tests were performed by Sellmeijer and a variety of colleagues on sandy soils in order to model seepage beneath structures (Sellmeijer and Koenders 1991, Weijers and Sellmeijer 1993). In Sellmeijer's experiments, defects in impervious boundaries or structures were modeled by

initiating flow through a sand bed beneath an impermeable barrier. This flow later exited the flume through a slit in the downstream portion of the flume. Tests were performed on varying hydraulic heads with observations made regarding the timing and initiation of piping erosion. Sellmeijer concluded that the critical hydraulic head was primarily a function of the permeability of the sand, and the particle size as characterized by D_{70}, the weight-percentage grain size diameter at which 70 percent of the soil by weight is finer (Weijers and Sellmeijer 1993).

Schmertmann (2000) also carried out flume experiments to model piping initiation along sloped soil surfaces. Schmetmann's results indicated a correlation between the gradients which initiated piping erosion, and the uniformity of the sand gradation measured using the coefficient of uniformity Cu.

Tomlinson and Vaid (2000) performed tests on spherical glass beads in order to determine the effects of confining pressure and seepage forces on the critical hydraulic gradient. They found that an increase in confining pressure resulted in an overall decrease in critical gradient. Their results also indicated that grain size ratio between the parent and filtration soil as well as the rapidity at which a gradient is applied can also affect the hydraulic gradient at which cohesionless soils may be prone to piping (Tomlinson and Vaid 2000).

Ojha, Singh, and Adrian (2001, 2003) have developed relationships relating the porosity and hydraulic conductivity of soils to the critical hydraulic gradient in under Darcy's Law assumptions. Their work indicates that using hydraulic conductivity relationships only related to grain-size diameter are not necessarily accurate for predicting critical hydraulic gradient; however use of Kozeny-Carman relationship which are a function of both the grain size and porosity are accurate (Ojha, Singh, and Adrian 2001, 2003).

Chang and Zhang (2013) recently investigated the effects of stress state on critical hydraulic gradients at which suffusion occurs in gap-graded soils. Suffusion is the erosion of finer particles from a matrix of coarser particles as a result of seepage flow (Chang and Zhang 2013). Tests were performed under drained triaxial conditions, isotropic, and triaxial extension conditions. They determined that the initiation of a critical hydraulic gradient is determined by the pore structure of the soil. Specifically as the stress ratio increases, porosity in the soil decreases. Therefore the gradient at which failure occurred was a function of the initial stress state of the soil, the applied seepage forces, and the shear strength of the soil with triaxial extension stress resulting in higher gradients for the initiation of piping (Chang and Zhang 2013).

Purpose

Using current analytic methods, the potential for piping failure to initiate is often analyzed using finite element analysis and comparing the results to a critical gradient. The critical gradient is often estimated from a simple relationship such as Equation 1. However as discussed in the previous paragraphs, this may not be accurate. Critical gradients in piping can depend on a variety of factors such as inherent properties of the soil including grain size, gradation, and porosity. The purpose of this study is to assess how a variety of these soil properties contribute to the overall initiation of the piping mechanism.

Fleshman and Rice (2013) developed a testing apparatus for evaluating the mechanisms associated with piping initiation in sandy soils and assessing the effects soil properties have on the critical hydraulic conditions needed to initiate piping. In their experiments they noted critical hydraulic conditions for initial movement, sand boil formation, and total heave occurrence. These phases of piping are discussed in greater detail throughout the paper. Testing was performed on a variety of sandy soils using the laboratory testing apparatus. A multi-variable

regression analysis was performed on the data which correlates the critical hydraulic gradient to the soil unit weight, friction angle, grain size characterized by D_{50} (the weight-percentage grain size diameter at which 50 percent of the soil by weight is finer), gradation characterized by the coefficient of uniformity, and void ratio. Friction angle was determined using angle of repose tests in order to best imitate the conditions of the soil under zero confining pressure, and during the progressive mounding and heave discussed in the Stages of Heave section of this paper.

Testing Methodology

Testing was performed in an apparatus designed to both control and measure the hydraulic pressure and gradients occurring in the soil sample as piping develops. A schematic of the testing apparatus can be seen in Figure 1. Sands are tested by placing them in a cylindrical apparatus with ports for measuring pore pressures located at distances of 0.75, 2.25, and 3.75 inches from the top of the container respectively. The soil container is 2-inches in diameter and 5-inches in length. It is made of Plexiglas with a screen at the base to allow water to flow through the sample while retaining the soil. The soil container is coated in silicon in order to prevent preferential flow paths from forming along the edges of the surface. Illustrations of the soil container can be seen in Figure 2. The silicon also allows for frictional interaction to occur between the soil and the container. Soils are placed into this container in 0.5 inch lifts. Each lift is densified by using a metal rod to sharply rap the side of the container.
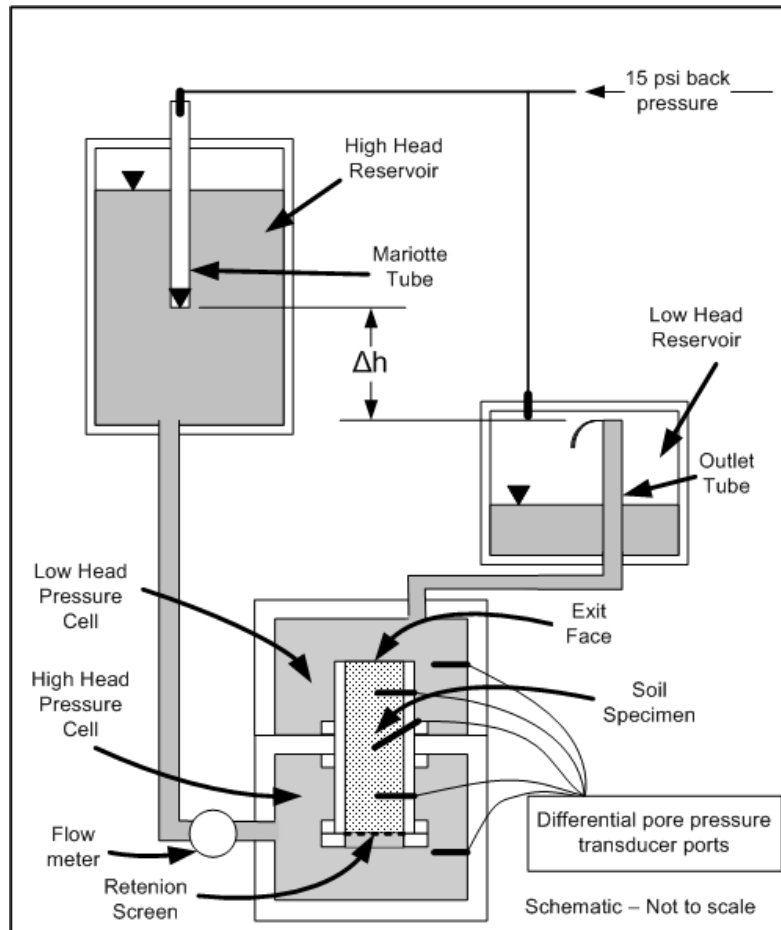
Figure 1: A schematic of the testing apparatus used in the testing methodology.[1]

[1] Image obtained from Fleshman and Rice (2013).

Figure 2: Soil container with ports for measuring pore pressures.

The sample holder is bolted and sealed vertically between two pressure cells housed in Plexiglas cylinder (Figure 3). The pressure cells are connected to reservoirs used to control and maintain the head across the sample holder.
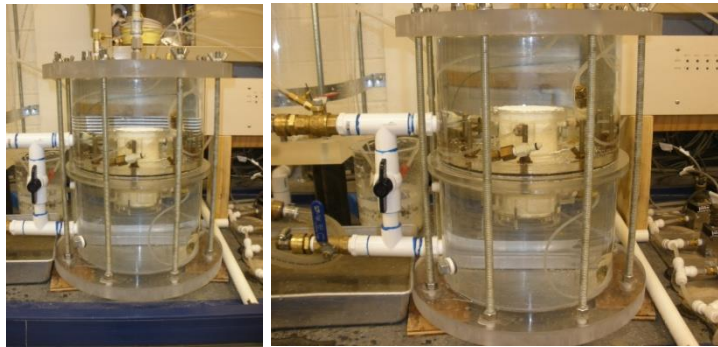

Figure 3: The pressure cell containing the soil container.

Carbon dioxide is introduced to the cell along with a vacuum for approximately 15 minutes to aid in de-airing the sample. The pressure cell is next filled with de-aired water and the sample is saturated from the top down while maintaining the vacuum on the pressure cells. Once the sample and pressure cells are completely filled, a back pressure of 15 psi is applied to the system using wall tanks. This constant back- pressure assists in saturation of the sample by forcing air bubbles into solution. Pressure head on the sample is increased from a beginning value of zero. The head was increased in small increments with observations of movement being made throughout testing.

The ports for measuring pore pressures are attached to Validyne DP15-26 differential pressure transducers. These pressure transducers provide readings to a demodulator (Figure 4) that calibrates the initial pressure across the soil sample. The pressure transducers are also linked to a data logger which collects data at one second time intervals throughout the test and provides graphical output of the differential heads of each transducer in units of inches of water (in H_2O). Flow is measured using a Kobold magnetic-flux flow meter. The flow-meter is linked to the data logger and graphical representations of flow data through the sample are also documented.
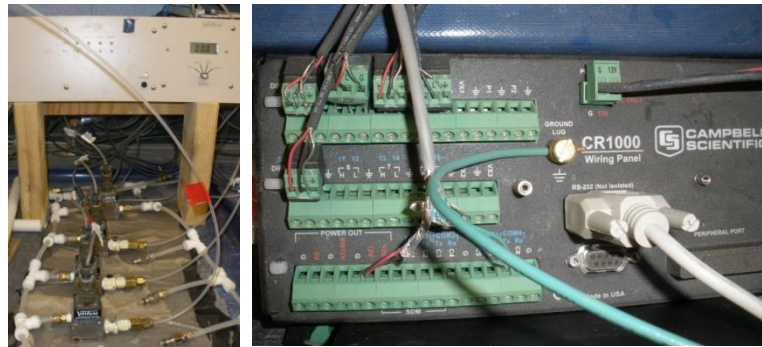
Figure 4: Pressure transducers attached to the demodulator (left) and the data collector (right).

Testing was also video recorded. A digital counter displays the time in seconds since the beginning of the test. These videos are then watched and times are recorded when initial movement, sand boil formation, and total heave, occur. These times can then be linked back to the data-logger output readings to determine exact head readings when each of these phenomenons occurs.

While pore pressure ports are spaced along the length of the sample and were used in previous studies to measure variation in head across the sample. They were not used in this analysis. Additional information regarding the methodology and apparatus used in this analysis is available in Fleshman and Rice (2013).

Testing was performed on a variety of sandy soils as well as zirconium beads. A summary of the materials tested as well as their respective properties can be seen in Table 1. Ottawa 20-30 and Graded sands conformed to the ASTM C778-03 standard. Angular silica sand in the same gradations as the Ottawa sands were also tested. Garnet sand was tested in order to compare the effects of unit weight on the sample. Zirconium beads were tested in a variety of gradations in order to compare the effects of grain size, and friction angle on critical hydraulic gradient.

Table 1: Table of the soil properties associated with each tested soil type.

Soil Type	Average Unit Weight (pcf)	Friction Angle (Degrees)[2]	Grain Size (D_{50} mm.)	Coefficient of Uniformity	Average Initial Void Ratio
Graded Angular	99.8	38	0.37	1.84	0.65
Angular 20-30	97.3	39	0.70	1.18	0.69
Garnet Sand	124.3	39	0.35	2	0.94
Graded Ottawa	111.3	35	0.37	1.84	0.48
Ottawa 20-30	111.9	35	0.70	1.18	0.47
Glass Beads 0.4-0.6 mm.	99.2	22	0.50	1.2	0.89
Zirconium Beads 0.3-0.4 mm.	154.3	24	0.35	1.2	0.33
Zirconium Beads 0.6-0.8 mm.	152.67	23	0.70	1.18	0.35
Graded Zirconium Beads	160.09	24	0.37	1.84	0.28

Stages of Heave

Fleschman and Rice identified four stages of piping development in their analysis. These include 1) first visible movement, 2) heave progression, 3) sand boil formation, and 4) total heave (Fleschman and Rice 2013). First visible movement, or stage one, is characterized by

---

[2] Friction angle was measured using angle of repose tests as mentioned in the Purpose section of this paper.

slight upward or vibratory movement of individual grains at the exit face. The head at which this first stage occurred was determined by repeated analysis of test video. The second stage, heave progression, is characterized by a downward progressing loosening of sand grains as the hydraulic gradient increases. As the loosening leads to an increase in void ratio, the seepage velocity correspondingly decreases. This leads to reduced viscous shear forces allowing more of the weight of the soil to be applied to the lower sections of the sample; resulting in equilibrium being achieved across the sample as hydraulic gradient increases. Visually, heave propagation was noted as a slow vertical mounding of soil along the exit face. Sand boil formation is typified by the formation of sand boils on the exit face. Sand boils form when preferential flow paths form throughout the sample. These flow paths form due to the random rearrangement of sand grains that occurs during the second stage. It is important to note that sand boils did not always form and that the second and third stages of piping often occur intermittently throughout the test. The fourth and final stage, total heave, occurs when the mounding at the exit face becomes unstable and begins to slough off the sides of the soil container. As the soil sloughs off of the sides, pressure is removed and the entire sample moves upward and heaves. (Fleschman and Rice 2013).

Results of Testing

The purpose of this analysis is to quantitatively link the previously discussed stages of piping with the following soil properties: unit weight, friction angle, grain size, uniformity, and initial void ratio. The critical gradients at each stage were plotted against the unit weight of the sample. These plots are documented in Figure 5. Included in this plot are values of critical hydraulic gradient, as well as a trend line indicating the lower bound values of measured hydraulic gradient with unit weight. A line indicating critical hydraulic gradient predicted using

Terzaghi's heave theory (Equation 1) is also included in Figure 5. These plots illustrate an obvious correlation between unit weight and critical hydraulic gradient. All measured unit weights are significantly above Terzaghi's predicted values. If we look at the lower bound values for each sample we can see that critical gradient generally increases with unit weight. However, there is also some variation in these trends as a result of the previously mentioned soil properties. This is especially true with regard to the 20-30 and graded angular sands. This effect is less apparent during Stage 1. The gradients for the angular soils are slightly above the overall trend including all of the soils. As heave progresses through Stage 3, the results become increasingly varied. The lowest gradients for the angular soils correspond with the trend of the other soils; however the higher gradients vary up to almost double the trend. At Stage 4 all of the gradients for the angular soils are above the trend line. These trends also points toward greater piping resistance in angular soils.

The effects of other soil parameters can also be seen in Figure 5, by contributing to the scatter of the plots. The effect of the coefficient of uniformity can clearly be seen. The critical gradients for more uniform, graded, soils are higher for similar unit weights. This trend continues throughout all stages of piping. It can then be inferred that more graded soils have greater piping resistance. The lower bound trends for each stage of piping indicate an increase in critical hydraulic gradient with unit weight. This indicates that the density, or specific gravity of the soils, contributing to the unit weight, also correlate to critical hydraulic gradient. Essentially, more dense soils or soils with a higher specific gravity show great piping resistance.

Figure 5: Plots of critical hydraulic gradient versus unit weight for three stages of piping.

The variation of results associated with the angular soils is likely due to interlocking of the grains along with an increased friction angle. During Stage 1, movement of the soil grains occurs in the uppermost layers of soil therefore minimizing the overall effects of the interlocking grains. Therefore, the results of the angular soils have less variation from the density trend in Stage 1. During Stage 3, sand boils form through preferential flow paths as a result of the random alignment of the interstitial voids. This random variation of the alignment of these interstitial voids occurs at a wider range of gradients for angular soils than occurs for soils with a rounder grain shape. This is because increased variation in the grain size and shape of angular soils will result in wider variation in the size and shape of the interstitial voids. As interstitial voids form, the smaller particles could also fill in these voids and further affect the size and shape of the preferential flow paths through the sample. In Stage 4 less variation between the gradients for angular soils exists, however the gradients are above the overall trend for the other soils. This is believed to be due to the increase in the angle of internal friction. This will increase bridging ability within the soil as well as the inclination of the heave mound prior to sloughing behavior.

Other Effects (Normalized Plots)

The effects of the angle of internal friction, grain size, uniformity, and void ratio, were initially analyzed by normalizing the critical hydraulic gradient with the critical hydraulic gradient predicted by Terzaghi using Equation 1. These normalized critical gradients were plotted against the previously mentioned soil properties. This indicates whether or not correlations exist between hydraulic gradient, unit weight, and the specified soil parameter. These plots also indicate how much of an effect the respective parameters are likely to have on predicting hydraulic gradient.

The normalized gradient plotted against the angle of internal friction is presented in Figure 6. These plots show a slight trend between the normalized hydraulic gradient and internal friction angle. This trend is not as steep during initial movement in Stage 1, but becomes more pronounced as piping progresses into Stage 3. This trend is maintained during total heave in Stage 4. Again the variation in the behavior of the angular soils is apparent within these plots. This behavior is again attributed to the random interlocking of soil particles resulting in variations in the alignment of interstitial voids and preferential flow paths. This trend is apparent throughout all of the normalized plots against the remainder of the soil properties.

The plots of normalized gradient versus grain size are presented in Figure 7. For the purpose of this experiment, grain size is characterized as the diameter at which 50% of the soil particles are finer by weight (D_{50}). The plots presented in Figure 6 indicate that grain size has very little observed effect. In Stage 1, a slightly negative effect can be seen. This changes to a slight positive trend but overall horizontal trend in Stage 3. This trend continues through Stage 4. Overall finer grained soils had a lower gradient to unit weight ratio than did coarser grained soils. If we look at all plots it can be inferred that coarse and fine soils reach similar values of critical hydraulic gradient. It is believed that during Stage 1, the loosening of the soil has not yet penetrated into the lower regions of the soil sample therefore the size of the grains has very little effect and the slight negative trend is likely a result of the effort needed to move the individual soil grains. As the loosening continues throughout the sample, this slight negative trend is offset as the grain size may affect the rearranging of the interstitial voids contributing to sand boil formation and eventually total heave of the sample.
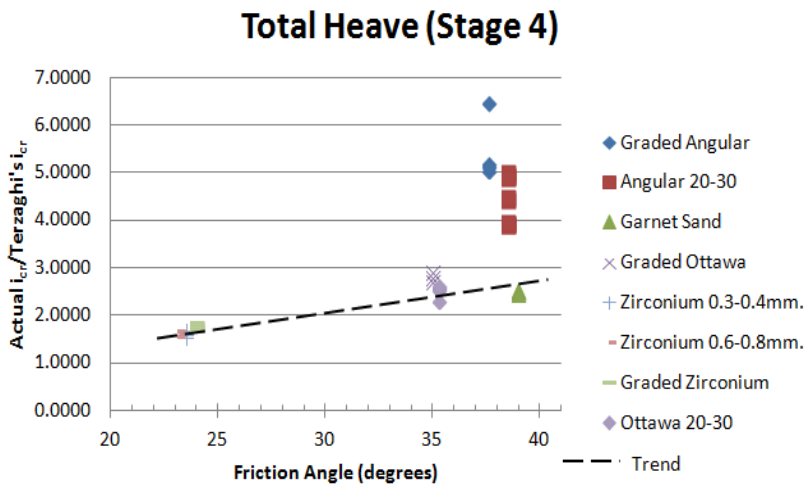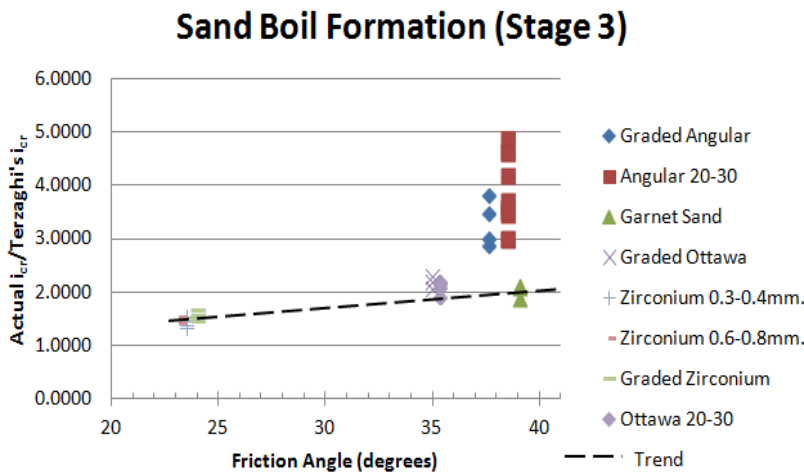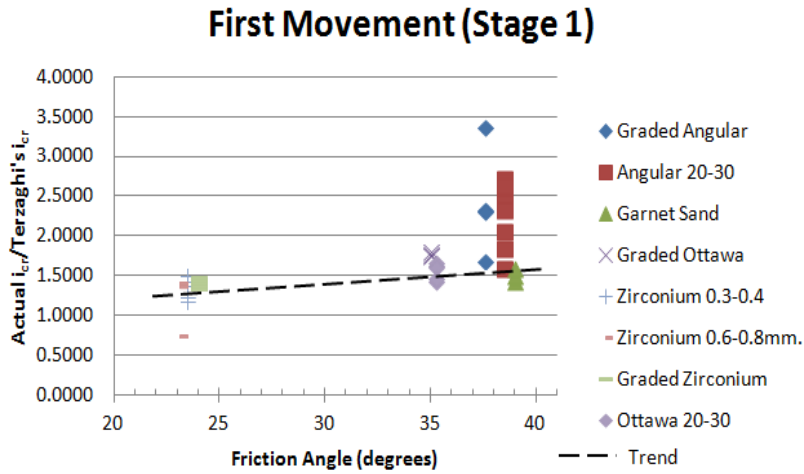
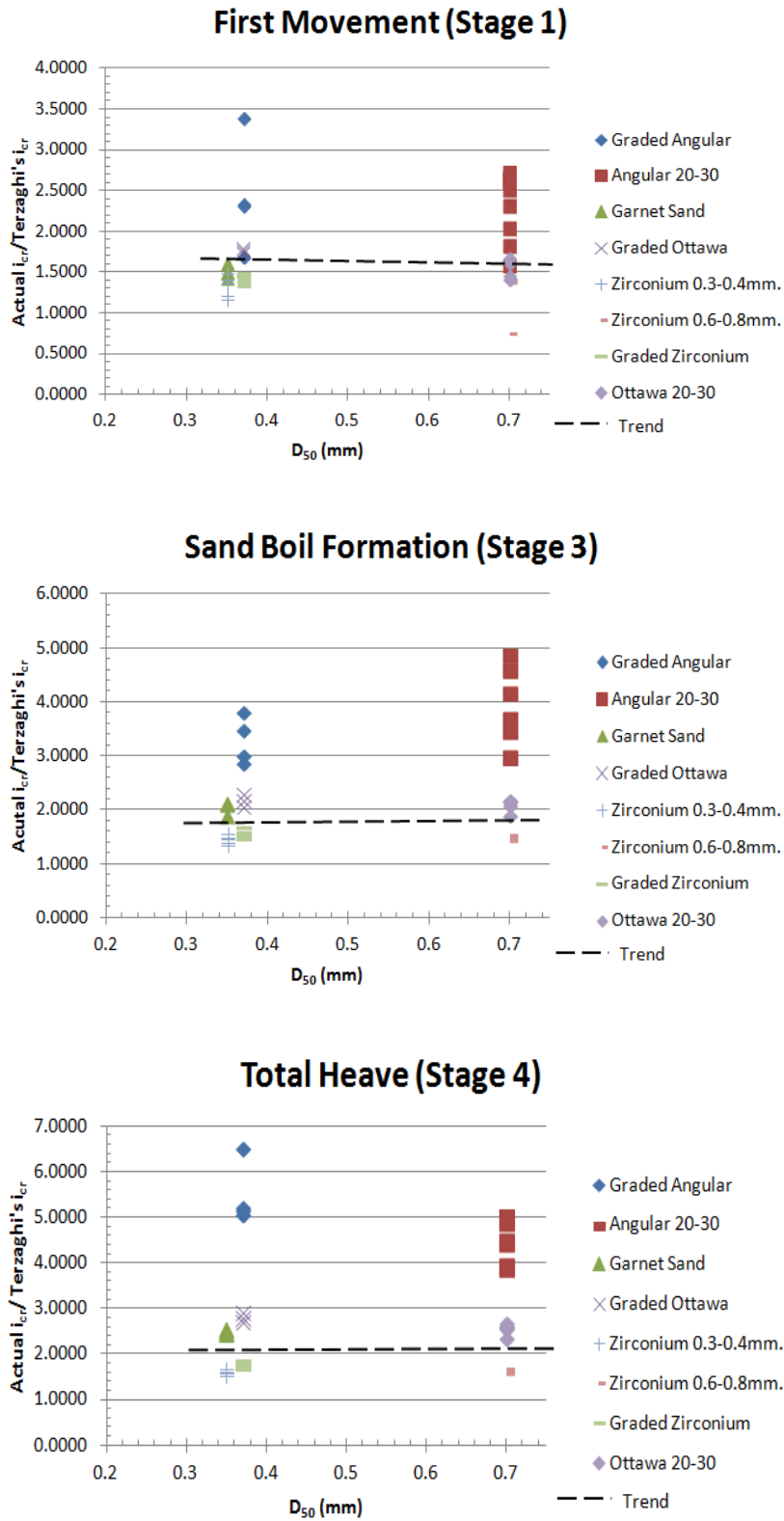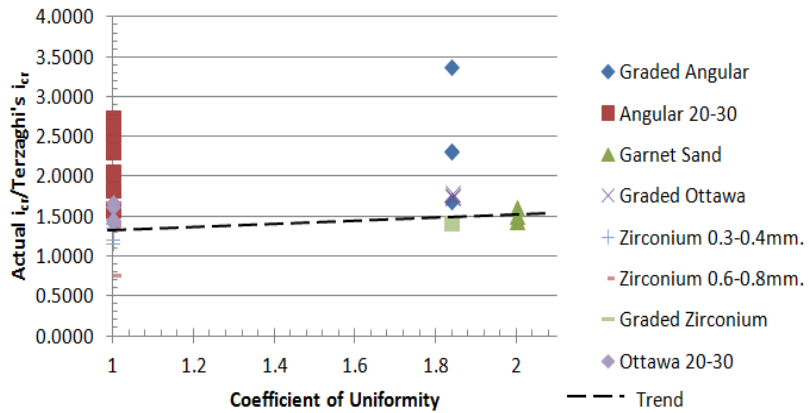**Figure 6:** Plots of normalized critical gradient versus the tangent of the friction angle.

Figure 7: Plots of normalized critical gradient versus grain size.

Normalized plots versus coefficient of uniformity can be seen in Figure 8. The coefficient of uniformity is a means of analyzing the result of gradation on piping. These plots illustrate that the ratio of critical gradient to unit weight generally increases with increasing coefficient of uniformity (more graded soils). This trend can be seen throughout each stage of piping. It is believed that the gradation of the soils affects the size of the interstitial voids within the sample. This would then affect the formation of the interstitial flow paths and the intergranular soil behavior.

The normalized plots versus initial void ratio can be seen in Figure 9. Similarly to the effects of grain size, void ratio has a slight negative trend during initial movement of the soil sample. The trend again becomes positive during sand boil formation. The trend remains positive and continues throughout Stage 4. The research and modeling performed by Fleshman and Rice indicates a loosening of the soil sample and an increase in void ratio as piping progresses. This would indicate that the negative effect void ratio would have on the sample would be during Stage 1, before the void ratio decreases with the downward progression of loosening throughout the soil sample. As this loosening progresses, the initial void ratio and orientation of the grains may have some affect on the formation of the interstitial voids, thus contributing to a slight positive increase in critical gradient with increasing void ratio.

Other attempts to normalize the data further with respect to the tangent of the angle of internal friction were also performed. However, these plots showed a large amount of scatter and showed little to no correlation between the various parameters therefore they are not discussed in this paper.
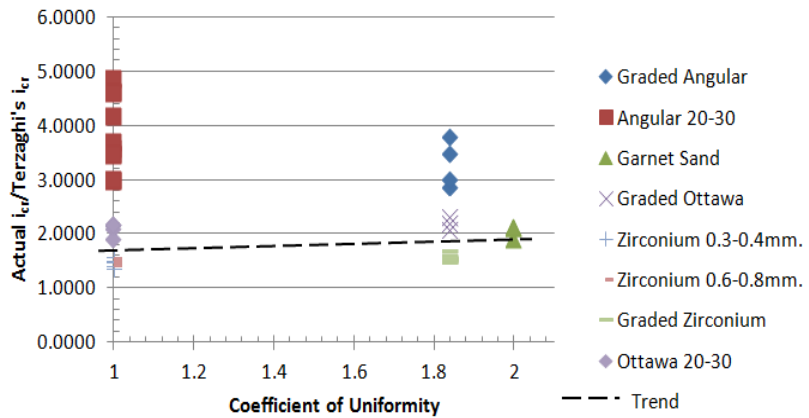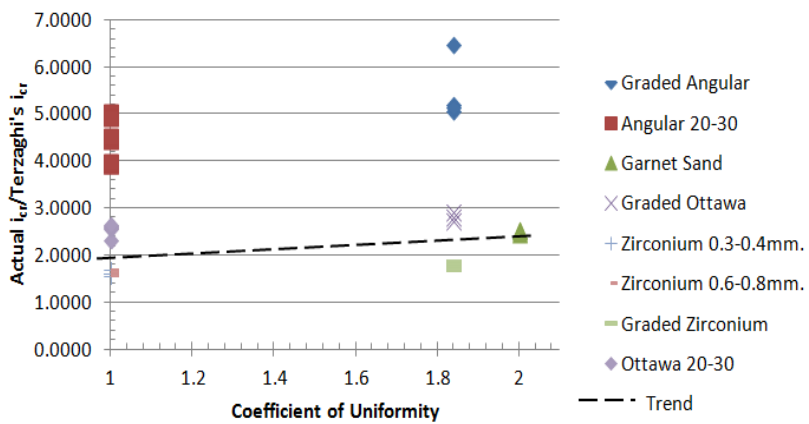
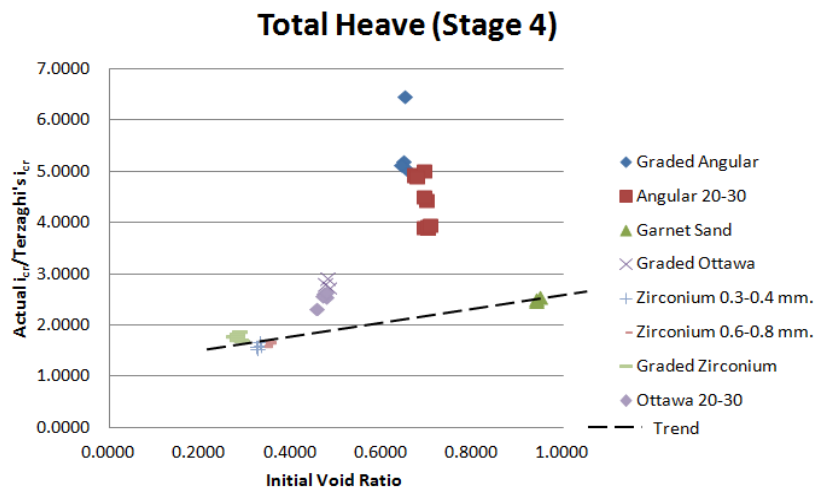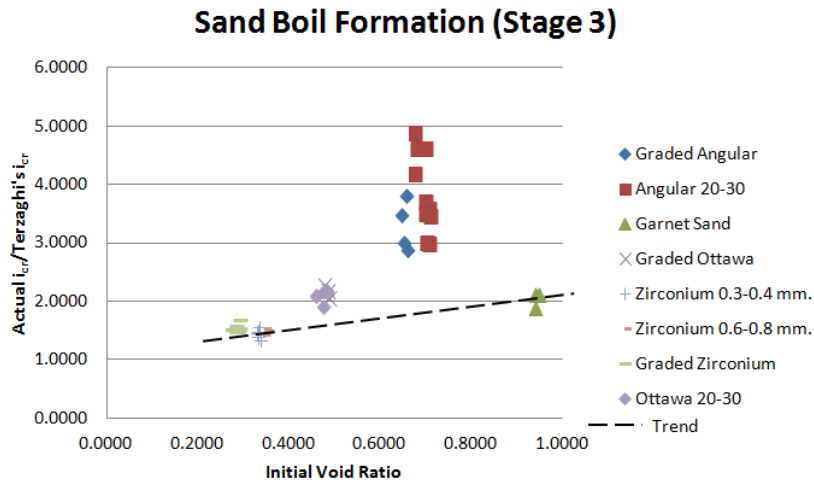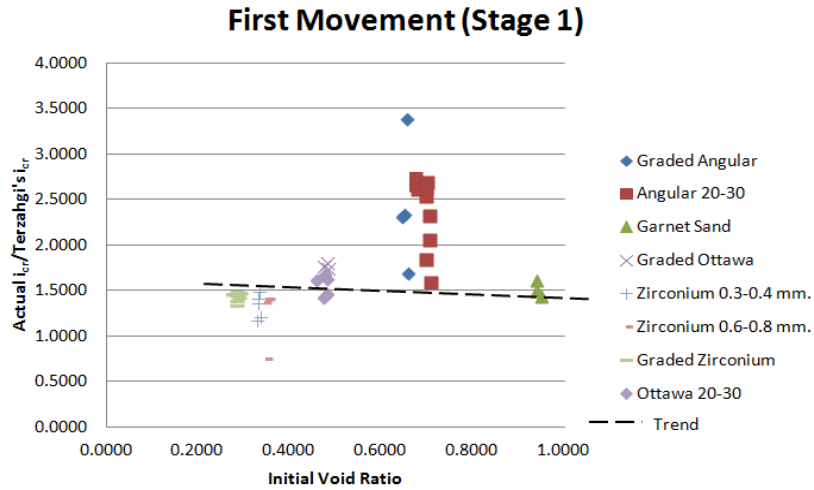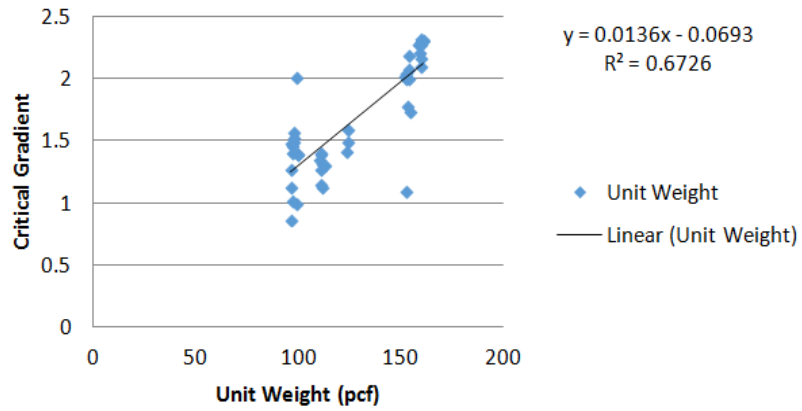**Figure 8:** Plots of normalized critical gradient versus coefficient of uniformity.

Figure 9: Plots of normalized critical gradient versus initial void ratio.
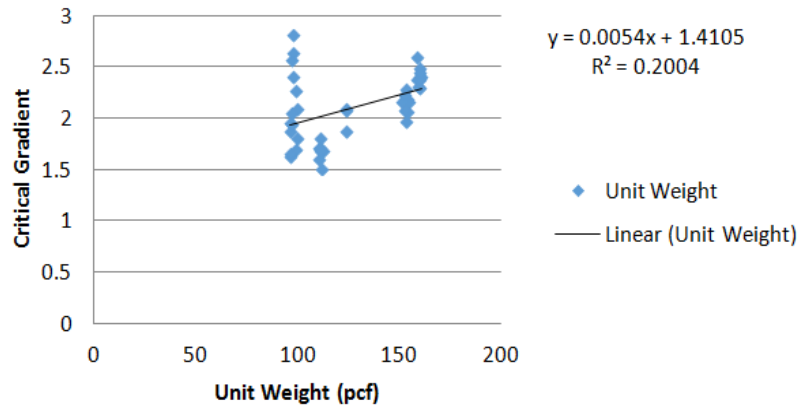
Multi-Variant Regression Analysis

To characterize the results of this testing, a multi-variable linear regression analysis was performed on the data. Linear, exponential, logarithmic, and power forms were considered for each of the soil parameters. However, because exponential, logarithmic and power equations demonstrate asymptotical behavior it was decided that these equation forms would not be applicable over a wider range of soil properties.

As can be seen from the plots in Figures 10 through 14, linear fit with individual parameters varied considerably across the different parameters and stages. Strength of the correlation was determined by R-square value. Overall, individual parameters fit better during Stage 1 and got worse as piping progressed. This is believed to be due to scatter in the angular soils. However this trend differed for the D_{50} and coefficient of uniformity. For the plots of D_{50} versus critical gradient, Stage 1 had the highest R-square correlation; however, the correlation for Stage 4 was stronger than the correlation for Stage 3. With coefficient of uniformity, it was found that Stage 4 had the strongest correlation while Stage 3 again had the lowest. This indicates that uniformity and grain size do not impact the critical gradient as much as other parameters during sand boil formation.

Initial Movement (Stage 1)

$y = 0.0136x - 0.0693$
$R^2 = 0.6726$

◆ Unit Weight

— Linear (Unit Weight)

Sand Boil Formation (Stage 3)

$y = 0.0054x + 1.4105$
$R^2 = 0.2004$

◆ Unit Weight

— Linear (Unit Weight)

Total Heave (Stage 4)

$y = 0.0008x + 2.4186$
$R^2 = 0.0036$

◆ Unit Weight
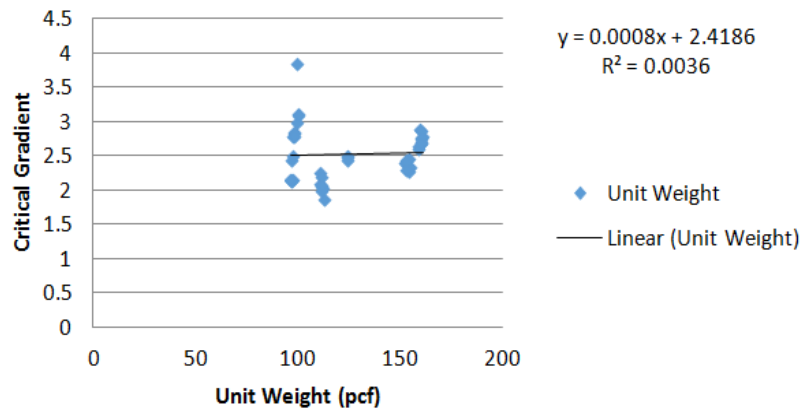
— Linear (Unit Weight)

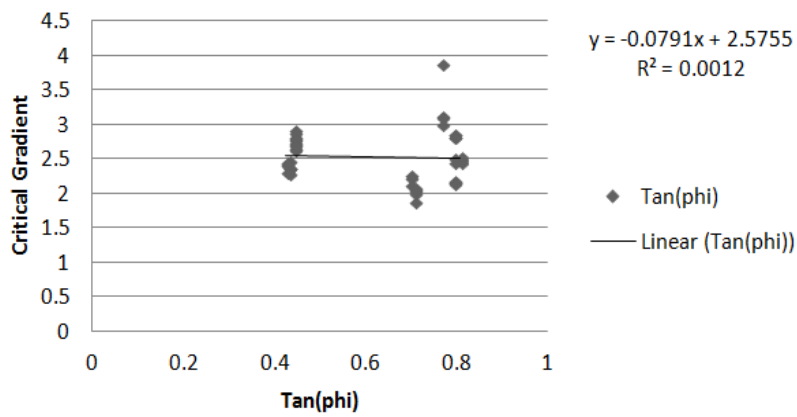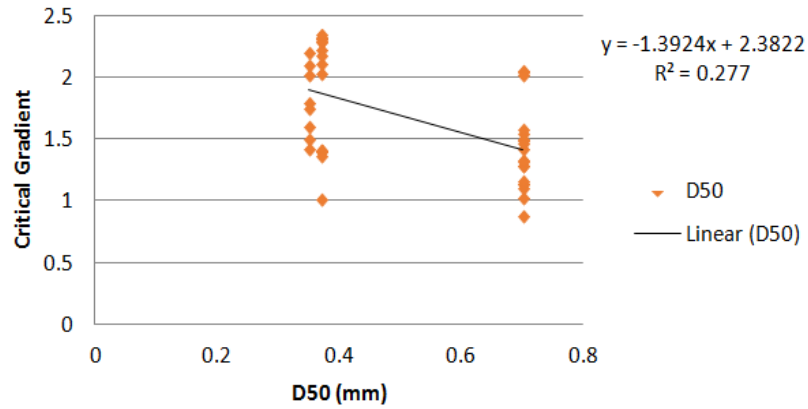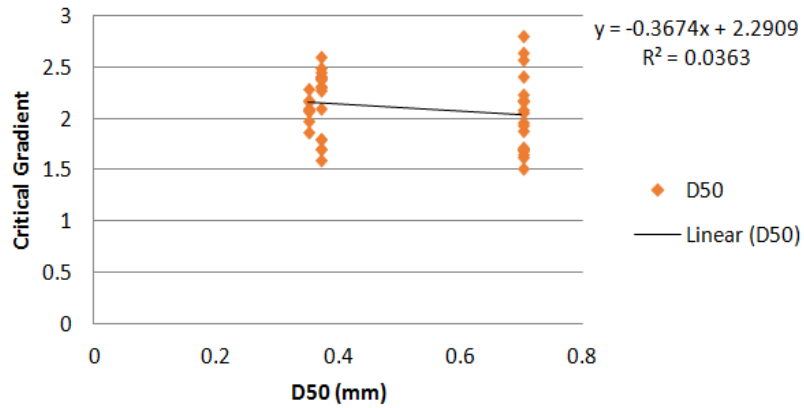**Figure 10:** Plots illustrating linear fit for gradient versus unit weight for each stage.

Figure 11: Plots illustrating linear fit for gradient versus the tangent of the angle of internal friction for each stage.

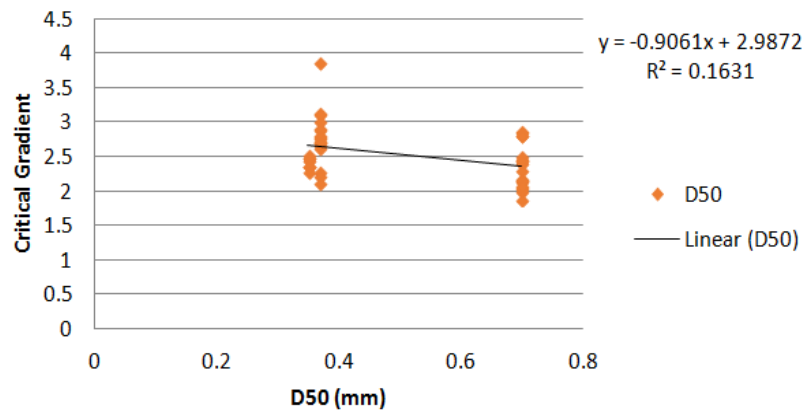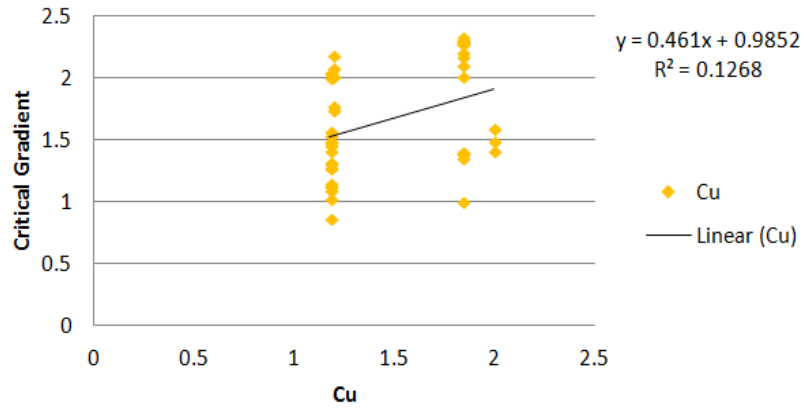**Figure 12:** Plots illustrating the linear fit for gradient versus grain size for each stage.

Initial Movement (Stage 1)

$$y = 0.461x + 0.9852$$
$$R^2 = 0.1268$$

◆ Cu

— Linear (Cu)

Sand Boil Formation (Stage 3)

$$y = 0.1464x + 1.8854$$
$$R^2 = 0.0241$$

◆ Cu

— Linear (Cu)

Total Heave (Stage 4)

$$y = 0.5357x + 1.7262$$
$$R^2 = 0.2379$$

◆ Cu
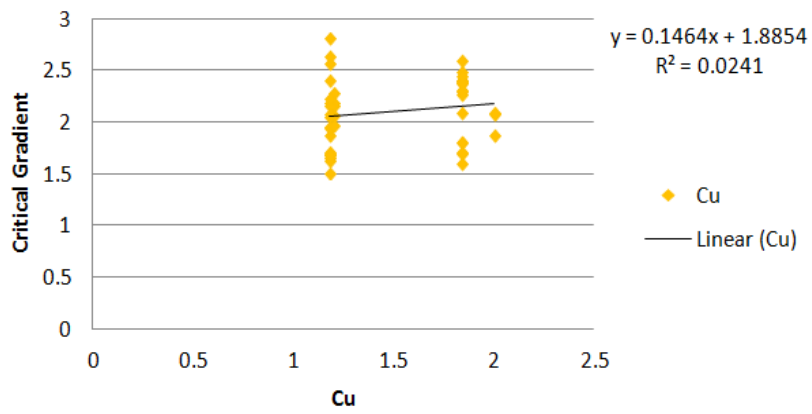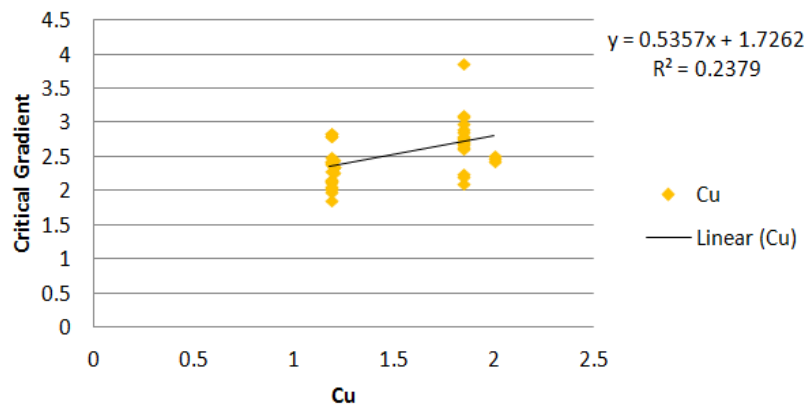
— Linear (Cu)

Figure 13: Plots illustrating the linear fit for gradient versus uniformity for each stage.
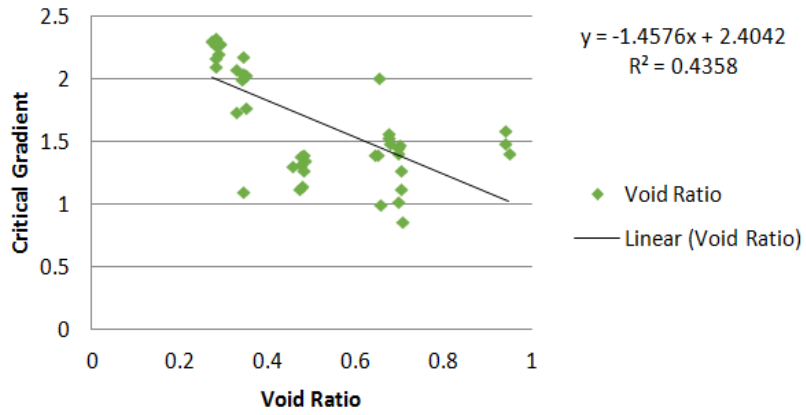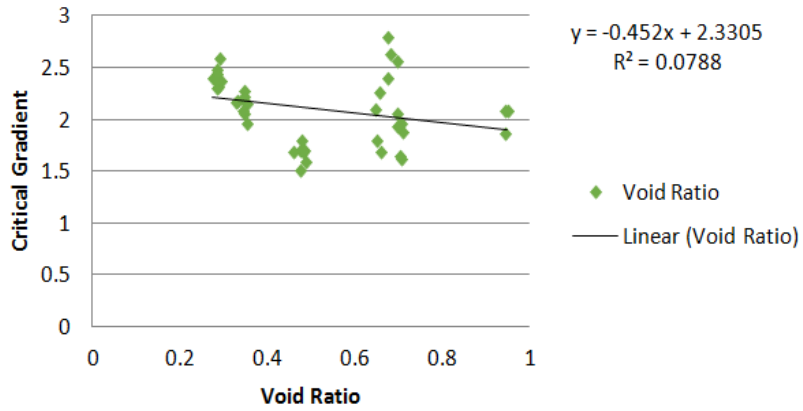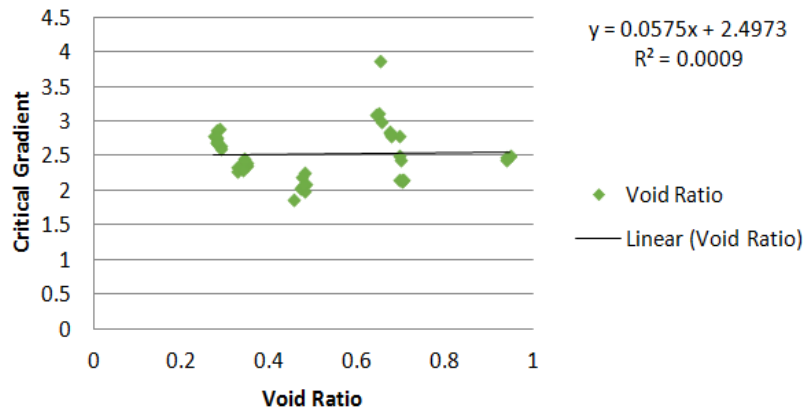
Figure 14: Plots illustrating the linear fit for gradient versus void ratio for each stage.

The best fit equations for Stages 1, 3, and 4 were modeled linearly after the form presented in Equation 2 where x signifies a given soil parameter and values of β are coefficients. The coefficients were determined using a regression in Microsoft Excel. The best fit equations determined using this analysis for Stage 1, 3, and 4 of piping can be seen in Equations 3 through 5 respectively.

$$A = \beta_0 + \beta_1 * x_1 + \beta_2 * x_2 + \ldots + \beta_n * x_n \tag{2}$$

$$i_{cr} = 0.014 * \gamma + 0.68 * \tan(\phi) - 0.059 * D_{50} + 0.20 * C_u - 0.52 * e - 0.52 \tag{3}$$

$$i_{cr} = 0.00041 * \gamma - 1.82 * \tan(\phi) + 0.53 * D_{50} + 0.27 * C_u + 0.85 * e + 2.09 \tag{4}$$

$$i_{cr} = -0.034 * \gamma - 7.56 * \tan(\phi) + 0.18 * D_{50} + 0.99 * C_u + 2.11 * e + 8.97 \tag{5}$$

In these equations γ is the initial unit weight of the sample in units of pounds per cubic foot., ϕ is the angle of internal friction, D_{50} is the diameter in millimeters of the soil particles where 50% of the soil is finer by weight, C_u is the coefficient of uniformity of the sample, and e is the initial void ratio of the sample.

The R-square value for Equation 3 (Stage 1) is 0.72. The R-square value for Equation 4 (Stage 3) is 0.24. The R-square value for Equation 5 (Stage 4) is 0.41. Plots of the observed critical gradients versus the critical gradients predicted using Equations 3 through 5 for each soil type are presented in Figure 15. A linear deviation trend line as well as a line representing a 1:1 correlation, or a perfect fit line, is also included in Figure 15 in order to better illustrate the precision of the equations. From these plots and the R-square values it can be seen that the best fit is achieved by Equation 3 for Stage 1, initial movement of the sample. This was expected due to the more linear trends of the individual soil parameters. This was also observed in the normalized plots. When the critical gradient was normalized and plotted against the individual

soil parameters, wide variation occurred in the critical gradient values for the angular soil samples. This variation was consistently at its minimum during Stage 1.

It is thought that the random interlocking of the angular soil particles to form interstitial voids and preferential flow paths plays more of an effect during Stages 3 and 4. This is because increased flow through the sample along with greater movement of the particles as piping progresses contribute to this variation. During Stage 1, the inter-particle behavior seen in Stages 3 and 4 is not as great, so the behavior of the angular soils is less prominent for initial movement.

Variation between the measured and predicted critical hydraulic gradients is also quantified by comparing the difference between the measured and predicted gradients (Δ) (i.e. the distance from the measured point to the 1:1 line), and the percent variation from the measured and predicted gradients. The absolute values of these parameters were also compared. Comparisons of the average Δ values and percent variations for each stage are presented in Table 2. This table illustrates that while Equation 3, for predicting hydraulic gradients for initial movement, has the most accurate R-square value; it also has the largest percent variation. Stage 1 also shows the least amount of difference determined using the absolute value of the difference between measured and predicted gradients (Δ). It is important to note that for perfect fit, the absolute value of this Δ should be zero. Stage 4 has the lowest percent variations. Stages 3 and 4 have significantly lower R-square values and higher differences (also determined based on absolute values) between measured and predicted gradients. Figure 15 and Table 2 illustrate that although Stages 3 and 4 do have larger scatter based upon R-square and Δ values, the percent variations are lower due to higher overall gradients. Much of the variation between measured and predicted values is the result of scatter from the intergranular behavior of the angular soils.
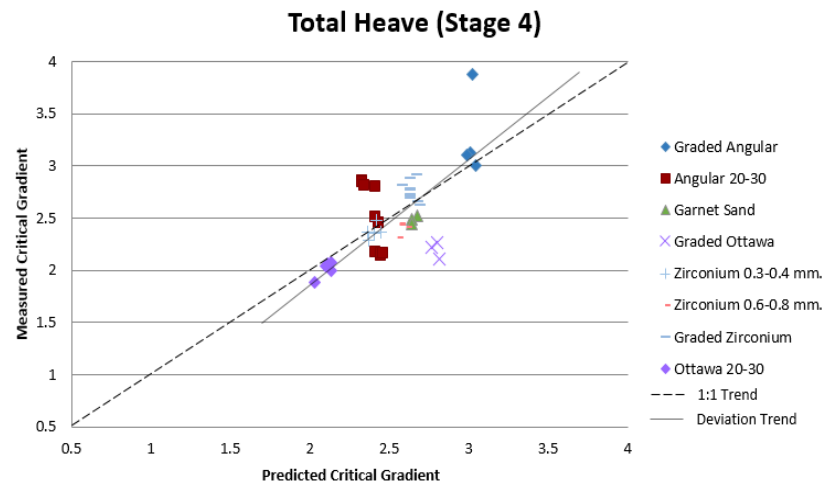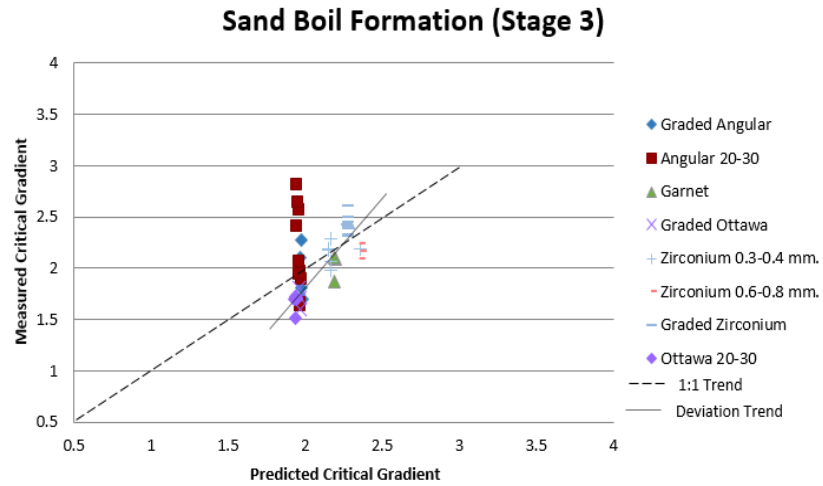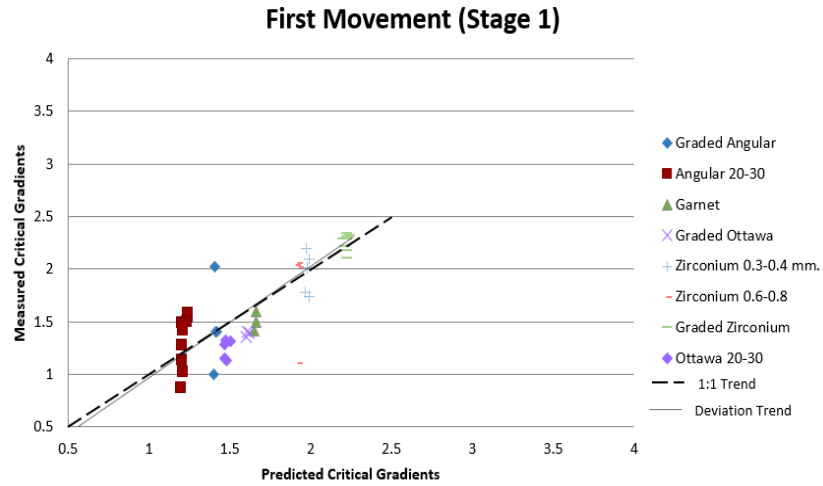
Figure 15: Plots of observed versus calculated values for each test.

Table 2: Table of variations between observed and calculated critical hydraulic gradients.

Stage	R^2	Average Δ	Average |Δ|	Average % Variation	Average |% *Variation*|
1	0.72	0.00	0.19	-2.33	13.3
3	0.24	0.00	0.22	-0.00	10.6
4	0.41	0.00	0.21	-1.18	8.26

Each of the soil types are more pronounced in Figure 15. This illustrates that the best fit equations would be more applicable for different soil types. For example, during Stage 1, the best fit equation predicts representative values for the zirconium beads regardless of grain size or gradation. A good fit for the zirconium beads can be seen throughout each stage. In Stages 3 and 4, a good fit is also apparent for Ottawa 20-30 soils.

In order to measure the effect each of the soil parameters had on the characteristic equations for each stage, the t-statistic ratio was used. The t-statistic ratio (t-stat) is the ratio between a coefficient β_n and its standard error. Therefore t-stat values provide a good indication of how much effect a parameter has on the variation of a characteristic equation. A comparison of the t-stat values for each parameter for each stage of piping is presented in Table 3.

It can be seen that for Stage 1, the unit weight clearly has the highest effect on critical gradient; in fact for Stage 1 every soil parameter has a significant impact on the predicted critical gradient except for grain size. This is reversed in Stage 3 where the impact of every parameter, especially unit weight, decreases and grain size becomes the dominant soil property. When piping progresses to Stage 4, the role of grain size is again diminished while the impact of all other soil properties again increases. These tendencies can also be seen in the plots in Figure 5. Important to note is the large impact the angle of internal friction has on predicting critical gradient during Stage 4. This is because of the mounding behavior exhibited during Stage 4, and to a lesser extent in Stage 1. Figure 6 also illustrates this behavior as the trend between

normalized critical gradient and angle of internal friction is at its greatest during Stage 4. A

similar behavior is seen in Figure 8 in which the correlation between normalized gradient is more

apparent during Stages 1 and 4.   Table 3 as well as Figure 9 also illustrate the consistency of the

void ratio in affecting critical gradient.

Table 3: A comparison of t-stat values for each soil property at each stage of piping.

Soil Parameter	t-Stat Values		
	Stage 1	Stage 3	Stage 4
Unit Weight (γ)	3.56	0.04	-3.32
Angle of Internal Friction ($\tan(\varphi)$)	1.14	-0.81	-3.27
Grain Size (D_{50})	-0.15	0.99	0.33
Uniformity (Cu)	1.10	0.98	3.50
Void Ratio (e)	-1.57	1.10	2.67

Summary and Conclusions

This paper discusses the results of a quantitative analysis on the effects of a variety of soil

parameters on the initiation of various stages of piping progression. Namely these soil

parameters were unit weight, angle of internal friction, grain size, gradation, and void ratio.

Testing was performed on a variety of soil samples with varying soil parameters using the

methodology used by Fleshman and Rice (2013). Equations were generated for the three stages

identified by Fleshman and Rice (2013): initial movement (Stage 1), sand boil formation (Stage

3), and total heave (Stage 4) in the progression of piping through a soil. Equations linking critical

hydraulic gradients to these soil properties were formed using a multi-variable linear regression

analysis.

Normalized plots indicated that the highest correlation existed between the unit weight, or density, of the soil sample and critical hydraulic gradient. This correlation appeared to be linear however the angular soils tested consistently had wider variation in critical hydraulic gradients than did the other soil samples. This variation peaked during Stage 3, and while there was less variation in Stage 4 all of the critical gradients were significantly higher than the overall trend for the other soil samples. This is likely due to the interlocking of the angular soil particles and an increased friction angle.

The highest qualitative correlation between critical hydraulic gradient and the listed soil parameters appears to occur for initial movement of the sample. This is illustrated by the low deviation as seen in Figure 15, although percent variation shows an opposite trend. Although deviation from perfect fit is greater for Stages 3 and 4, percent variation indicates better fit for these stages. This correlation is likely because the progressive loosening of the soil and increase in void ratio across the sample as piping progresses has not occurred at the degree seen in sand boil formation and total heave. Although deviation from perfect fit is greater for Stages 3 and 4, percent variation indicates better fit for these stages. Increased deviation is likely due to the behavior of the angular soils as well as the changes in density and void ratio across the sample as piping progresses.

Based upon this analysis, it is recommended that critical hydraulic gradients be predicted using the lower bound trend represented in Figure 5. This will give a conservative estimate in order to account for the scatter found in the qualitative equations, while providing a more accurate representation of piping occurrence than Terzahgi's theory of heave equation.

Acknowledgements

References

Bligh, W.G. ,1910, "Dams, Barrages, and Weirs on Porous Foundations," *Engineering News* 64(26), 708-710.

Bligh, W.G. , 1913, "Lessons from the Failure of a Weir and Sluices on Porous Foundations," *Engineering News*, 69(6), 266-270.

Chang, D.S. and Zhang, L.M., 2013, "Critical Hydraulic Gradients of Internal Erosion under Complex Stress States" *Journal of Geotechnical and Geoenvironmental Engineering.* 139(9) pp.1454-1467

Fleshman, M. and Rice, J., 2013, "Constant Gradient Piping Test Apparatus for Evaluation of Critical Hydraulic Conditions for the Initiation of Piping", *ASTM Geotechncial Testing Journal*, 36(6), pp 1-14.

Fleshman, M. and Rice, J., 2013, "Laboratory Modeling of the Mechanisms of Piping Erosion Initiation", *Journal of Geotechnical and Geoenvironmental Engineering*, GTENG-3418R1.

Foster, M., Fell, R., and Spannagel, M., 2000, "Statistics of embankment dam failures and accidents," *Canadian Geotechnical Journal*, 37(5), pp. 1000-1024.

ICOLD (International Committee on Large Dams), 2012, "Internal Erosion of Existing Dams, Levees, and Dikes, and their Foundations", *ICOLD Bulletin IXX*, Draft of May 21, 2012

Ojha, C.S.P., Singh, V.P., and Adrian, D.D., 2001, "Influence of Porosity on Piping Models of Levee Failure" *ASCE Journal of Geotechincal and Geoenvironmental Engineering*, Vol. 127(12), pp. 1071-1074.

Ojha, C.S.P., Singh, V.P., and Adrian, D.D., 2004, "Determination of Critical Head in Soil Piping", *ASCE Journal of Geotechincal and Geoenvironmental Engineering*, Vol. 127(12), pp. 1071-1074.

Richards, K.S. and Reddy, K.R., 2007, "Critical appraisal of piping phenomena in earth dams," *Bulletin of Engineering Geology and the Environment*, 66(4), pp. 381-402.

Schmertmann, J.H., 2000, "The Non-Filter Factor of Safety Against Piping Through Sand" *ASCE Geotechnical Special Publication No. 111, Judgment and Innovation,* Edited by F. Silva and E. Kavazanjian, ASCE, Reston, VA, pp. 65-132.

Sellmeijer, J.B. and Koenders, M.A., 1991, "A Mathematical Model for Piping", *Applied Mathematical Modeling*, Butterworth-Heinemann, Vol.115, pp.646-661.

Terzaghi, K., 1922, "Der Grundbruch an Stauwerken und Seine Verhutung [The Failure of Dams and Its Prevention]," *Die Wasserkraft*, Vol. 17, pp. 445-449.

Terzaghi, K., 1939, "Soil Mechanics: a new chapter in engineering science," *J. Instn Civ Eng,* Vol. 12, pp.106-141.

Terzaghi, K., 1943, *Theoretical Soil Mechanics*. Wiley, New York, 510 p.

Terzaghi, K., and Peck R. B. (1948). *Theoretical Soil Mechanics in Engineering Practice*. Wiley, New York.

Tomlinson, S. S. and Vaid, Y. P., 2000, "Seepage Forces and Confining Pressure Effects on Piping Erosion", *Canadian Geotechincal Journal*, Vol. 37, pp. 1-13.

Weijers, J.B.A and J.B. Sellmeijer, 1993 "A New Model to Deal with the Piping

Mechanism on Filters, in Geotechnical and Hydraulic Engineering", In *Filters in Geotechnical*

and,Hydrauilc Engineering, Brauns, Herbaum and Schuler (editors), Balkema, Rotterdam, pp.

349-355.